 doi:10.20944/preprints202012.0376.v1

Antidepressant drug enhanced TRAIL receptor-2 expression and sensitized lung cancer cells to TRAIL-induced apoptosis via Inhibition of autophagic flux

K.M.A. Zinnah[1,2], Jae-Won Seol[1], and Sang-Youel Park[1,*]

[1]*Biosafety Research Institute, College of Veterinary Medicine, Jeonbuk National University, Gobong ro, Iksan, Jeonbuk 54596, South Korea*

[2]*Faculty of Biotechnology and Genetic Engineering, Department of Animal and Fish Biotechnology, Sylhet Agricultural University, Sylhet-3100, Bangladesh*

***Corresponding author:**
Sang-Youel Park
Biosafety Research Institute, College of Veterinary Medicine, Jeonbuk National University
Gobong ro, Iksan, Jeonbuk 54596, South Korea
E-mail: sypark@chonbuk.ac.kr
Tel: 82-63-850-0966; Fax: 82-63-850-0910

Running title: DESIPRAMINE ENHANCED TRAIL-INDUCED APOPTOSIS IN LUNG CANCER CELLS

 doi:10.20944/preprints202012.0376.v1

Abstract

Autophagy, an alternative cell death mechanism, is also termed programmed cell death type II. Autophagy in cancer treatment needs to be regulated. In our study, autophagy inhibition by desipramine or the autophagy inhibitor chloroquine (CQ) enhanced tumor necrosis factor-related apoptosis-inducing ligand (TRAIL) receptor-2 [death receptor (DR5)] expression and subsequently TRAIL-induced apoptosis in TRAIL-resistant A549 lung cancer cells. Genetic inhibition of DR5 substantially reduced desipramine-enhanced TRAIL-mediated apoptosis, proving that DR5 was required to increase TRAIL sensitivity in TRAIL-resistant cancer cells. Desipramine treatment upregulated p62 expression and promoted conversion of light chain 3 (LC3)-I to its lipid-conjugated form, LC3-II, indicating that autophagy inhibition occurred at the final stages of autophagic flux. Transmission electron microscopy analysis showed the presence of condensed autophagosomes, which resulted from the late stages of autophagy inhibition by desipramine. TRAIL, in combination with desipramine or CQ, augmented the expression of apoptosis-related proteins cleaved caspase-8 and cleaved caspase-3. Our results contributed to the understanding of the mechanism underlying the synergistic anti-cancer effect of desipramine and TRAIL and presented a novel mechanism of DR5 upregulation. These findings demonstrated that autophagic flux inhibition by desipramine potentiated TRAIL-induced apoptosis, suggesting that appropriate regulation of autophagy is required for sensitizing TRAIL-resistant cancer cells to TRAIL-mediated apoptosis.

Key words: Desipramine; Autophagy; Apoptosis; Death receptor-5; TRAIL

 doi:10.20944/preprints202012.0376.v1

1. Introduction

Lung cancer is a common cause of cancer-related deaths [1]. Among the cancers diagnosed in the USA in 2018, lung cancer ranked second in terms of incidence rate [2]. Every year, 1.6 million people die of lung cancer, and 1.8 million people are newly diagnosed. After diagnosis, the 5-year survival rate is 4-17%, which varies based on the stage of the cancer [3]. Various treatment strategies include targeted chemotherapeutic agents, surgery, and radiotherapy for the treatment of advanced non-small cell lung cancer [4]. Newer approaches such as specific combination strategies with potential chemotherapeutic drugs may be a good choice for cancer treatment [5].

Tumor necrosis factor-related apoptosis-inducing ligand (TRAIL) is a transmembrane cytokine that has shown the prospect of being used successfully for cancer treatment [6]. It can selectively kill a wide range of tumor cells with no or minimal toxic effects on normal cells [7]. TRAIL-mediated cancer cell killing can occur via both extrinsic and intrinsic apoptotic pathways. TRAIL binds to its receptors, death receptor 4 (DR4) and DR5, prompting apoptotic signals [8]. Subsequently, recruitment of the Fas-associated death domain (FADD) protein and, eventually, procaspase-8 by the FADD protein activates the death-inducing signaling complex (DISC), leading to the activation of caspases-8 and -9 and then the effector caspases-3, -6, and -7. This then results in membrane blebbing, DNA fragmentation, and nuclear shrinkage [9, 10]. Although TRAIL is unique for its cancer cell killing capacity, various cancer cells are resistant to TRAIL [11, 12]. A large number of tumor cells including human A549 lung cancer cells are resistant to the apoptotic effects of the TRAIL signaling pathway [13, 14]. Study has shown that it is possible to overcome TRAIL resistance using effective TRAIL-sensitizing agents [15].

Autophagy, an alternative cell death mechanism, is also named programmed cell death type II [16]. Autophagy eliminates cytosolic components and damaged or misfolded proteins using a lysosome-mediated degradation system, which is promoted under stress conditions such as starvation, hypoxia, growth factor deprivation, and endoplasmic reticulum stress [17]. Autophagic flux is the complete mechanism of autophagy wherein cytosolic components are sequestered into double-membrane vesicles, autophagosomes, which subsequently fuse with lysosomes, initiating the degradation and recycling of these cytosolic components [18]. The formation of autophagosomes is indicated by the conversion of the microtubule-associated protein, light chain 3 (LC3)-I, to its lipid-conjugated form, LC3-II, which is commonly

 doi:10.20944/preprints202012.0376.v1

considered a marker of complete autophagosome formation [19]. The autophagosome then combines with lysosomes. p62 (SQSTM1), a ubiquitin-like lysosomal protein, which is incorporated into the autophagosome, degrades LC3-II and additional cargo proteins. Thus, inhibition of autophagy results in increased p62 protein levels [20, 21]. Autophagy functions as a mechanism of tumor suppression during tumor formation processes and has been reported to promote tumor cell survival after tumor formation. Thus, autophagy is like a double-edged sword [22]. Many studies have shown that autophagy can play a cell protective role by carrying energy throughout metabolic stress and help avoid cancer cell death [23, 24]. Recent studies revealed that pharmacological or genetic inhibition of autophagy enhanced cancer cell death during chemotherapy, indicating that autophagic flux inhibition might be a suitable and promising strategy for cancer treatment [25-27]. For example, chloroquine (CQ), or related hydroxychloroquine (HCQ), is an autophagy inhibitor that prevents acidification of lysosomes, inhibits fusion of autophagosomes with lysosomes, and augments the apoptotic effect [28-30].

Antidepressants are commonly recommended for the treatment of depression, psychiatric disorders, and chronic pain in cancer patients [31]. For example, desipramine is a tricyclic antidepressant (TCA) that is used as a first-line drug for the treatment of neuropathic pain [32]. As a member of the TCA class of drugs, desipramine has shown cytotoxic effects in many cancer cell lines such as human MG63 osteosarcoma cells [33], human HT29 colon carcinoma cells [34], human PC3 prostate cancer cells [35], C6 glioma cells [36], and mouse Ca3/7 skin squamous cells [37]. However, the anti-cancer effect of desipramine on lung cancer cells has not been reported yet. Therefore, we aimed to investigate the role of desipramine treatment in lung cancer.

In the present study, we demonstrated that inhibition of autophagic flux by desipramine enhanced TRAIL-induced A549 lung cancer cell death and activated DR5. Single treatment with either desipramine or TRAIL did not affect cell death. Although A549 cells are TRAIL-resistant, desipramine treatment enhanced DR5 expression. Co-treatment of desipramine and TRAIL exhibited a stronger effect on A549 lung adenocarcinoma cells than monotherapy with either desipramine or TRAIL.

Preprints (www.preprints.org) | NOT PEER-REVIEWED | Posted: 15 December 2020 doi:10.20944/preprints202012.0376.v1

2. Results

2.1. Effects of desipramine treatment on TRAIL-induced death of lung cancer cells

To study the combined effect of desipramine and TRAIL on the inhibition of lung cancer cell viability, we used the A549 lung cancer cell line. The results demonstrated a strong combined effect on this cell line. Cells were preincubated with desipramine (30 μM) for 12 h and then co-treated with TRAIL (100 ng/mL) for 3 h. Cell morphologies and their changes were captured under a light microscope. Desipramine, in combination with TRAIL, increased apoptotic cell death (Figures 1A, B, E, F, I and J). MTT assay demonstrated that the combined treatment significantly inhibited growth in a dose-dependent manner (Figure 1C, G and K). The trypan blue exclusion assay showed that the combined treatment, compared to single treatment, robustly decreased the number of viable cells to a greater extent (Figure 1D, H and L). These results suggested that desipramine sensitized TRAIL-resistant A549 lung adenocarcinoma cells to TRAIL-mediated apoptotic cell death.

2.2. Combined desipramine and TRAIL treatment effectively inhibited the formation of A549 cell colonies and enhances TRAIL-mediated apoptosis

We further examined the combined effects of desipramine and TRAIL on the colony-forming capacity of A549 cancer cells. When A549 cells were cultured with desipramine (30 μM) for 3 days, colony formation was completely inhibited; thus, the desipramine dose was reduced to 15 μM. Single TRAIL or desipramine treatment slightly reduced colony formation, whereas combined TRAIL-drug treatment significantly reduced colony formation and size (Figures 2A, B). Annexin V results indicated combined treatment of desipramine and TRAIL augments apoptotic cell death than treatment with cell alone either desipramine or TRAIL (Fig. 2C, D). Collectively, these results confirmed that desipramine increased TRAIL-mediated apoptosis in TRAIL-resistant lung adenocarcinoma A549 cells.

2.3. Effects of TRAIL receptor-2 (DR5) on TRAIL-induced apoptosis

To understand the underlying molecular mechanism of apoptosis of A549 cells induced by combined treatment with desipramine and TRAIL, we investigated whether the expression of death receptors was related to TRAIL-induced apoptosis. TRAIL resistance in several cancer cells was found to be associated with downregulated expression of the TRAIL receptors DR4 and DR5 or upregulated expression of the decoy receptors DcR1 and DcR2. Western blot analysis showed that desipramine treatment enhanced DR5 expression in a dose- and time-

Preprints (www.preprints.org) | NOT PEER-REVIEWED | Posted: 15 December 2020 doi:10.20944/preprints202012.0376.v1

dependent manner but had no effect on DR4 expression (Figure 3A). Desipramine treatment also increased DR5 transcript levels (Figure 3B). Furthermore, ICC revealed substantially greater appearance of DR5 in desipramine-treated cells than in non-treated cells (Figure 3C). Finally, the apoptosis marker proteins, cleaved caspase-8 and cleaved caspase-3, were more markedly expressed after combined desipramine and TRAIL treatment than after single treatment (Figure 3D). Therefore, DR5 potentiation by desipramine is essential for TRAIL-induced apoptosis.

2.4. Suppression of DR5 altered the results of desipramine-induced TRAIL-mediated apoptosis

We applied DR5-specific siRNA to block DR5 expression, thereby restoring cancer cell viability. This finding provided evidence that DR5 plays an important role in augmenting the effect of desipramine on TRAIL-induced apoptosis. Cells, transfected with DR5-specific siRNA or negative control (NC) siRNA for 24 h and treated with desipramine for 12 h, were incubated with TRAIL for an additional 3 h for cell viability evaluation and an additional 2 h for western blot analysis. After siRNA transfection, the ability of desipramine, in combination with TRAIL, to induce cell death was reduced. However, the combined effect of desipramine and TRAIL on cell viability was similar in NC siRNA-transfected cells (Figures 4A, B, C). Western blot results showed that DR5-specific siRNA-transfected cells, compared to the non-transfected cells, showed blocked DR5 expression (Figure 4D). The upregulation of DR5 by desipramine demonstrated the important role of DR5 in attenuating TRAIL resistance.

2.5. Effects of desipramine treatment on autophagic flux

To identify the function of desipramine in autophagic flux, we checked the levels of the autophagy markers LC3-II and p62. Immunoblotting assay revealed that desipramine inhibited autophagy at the final stages of autophagic flux. Desipramine converted LC3-I to LC3-II, indicating the formation of complete autophagosomes, and increased p62 levels by inhibiting its degradation in lysosomes or proteasomes (Figure 5A). The genetic autophagy inhibitor atg5 did not alter the expression of p62 and LC3-II. Therefore, atg5-independent autophagosome accumulation occurred in desipramine-treated cells (Figure 5B). TEM exposed the condensed accumulation of autophagic vacuoles. This was absent in the control, thereby establishing that desipramine inhibited autophagic flux (Figure 5C). ICC analysis also revealed that autophagic flux inhibition by desipramine increased the expression level of p62 in a dose-dependent

Preprints (www.preprints.org) | NOT PEER-REVIEWED | Posted: 15 December 2020 doi:10.20944/preprints202012.0376.v1

manner (Figure 5D). These experiments indicated that desipramine inhibited autophagic flux by inhibiting autophagosome-lysosome fusion in lung cancer cells.

2.6. Autophagic flux inhibition upregulated DR5

To investigate the role of autophagic flux inhibition in DR5 expression, we used the autophagy inhibitor CQ. CQ inhibited autophagic flux and thus upregulated DR5 expression. Cell culture plates were pretreated with CQ (20 μM) or indicated doses of desipramine for 12 h. Immunoblotting assay showed that desipramine and CQ increased the levels of LC3-II. Moreover, desipramine alone enhanced p62 expression in a dose-dependent manner. These findings suggested that desipramine inhibited autophagic flux to induce apoptosis (Figure 6A). Furthermore, DR5 expression was upregulated in desipramine- and CQ-treated cells (Figure 6B). Finally, we checked the levels of apoptosis-related proteins cleaved caspase-8 and cleaved caspase-3. Desipramine or CQ, in combination with TRAIL, increased the levels of cleaved caspase-8 and cleaved caspase-3 (Figure 6C). Overall, these findings proved that autophagy inhibition enhanced TRAIL-mediated apoptosis by upregulating DR5 expression.

2.7. Autophagy inhibition by desipramine augmented TRAIL-induced cell death

To investigate the role of desipramine in autophagy inhibition and subsequent TRAIL-mediated cell death, a functionally active autophagy inhibitor CQ was applied. Cells were pretreated with CQ or desipramine at specified doses for 12 h and finally incubated with TRAIL for 3 h. Morphological analysis of cells by light microscopy and crystal violet assay revealed that A549 cells treated with either TRAIL or desipramine showed slight cell death, whereas cells treated with a combination of desipramine or CQ and TRAIL showed significantly improved TRAIL-mediated cell death (Figures 7A, B). MTT and trypan blue staining assays showed that cells treated with desipramine or CQ, in combination with TRAIL, demonstrated decreased cell viability and augmented cell death (Figure 7C). Collectively, these findings showed that desipramine enhanced TRAIL-induced apoptosis by inhibiting autophagic flux.

Preprints (www.preprints.org) | NOT PEER-REVIEWED | Posted: 15 December 2020 doi:10.20944/preprints202012.0376.v1

3. Discussion

Depression is the most common symptom in cancer patients, and it suppresses their anti-cancer immunity. The main purpose of our study was to investigate the function of desipramine and co-treatment of desipramine and TRAIL in A549 lung cancer cells. We found that desipramine inhibited autophagic flux, resulting in DR5 upregulation, which finally enhanced TRAIL-induced apoptosis of A549 cells.

TRAIL is a transmembrane cytokine and shows promising anti-cancer activities in tumor cells without cytotoxic effects. Since it is a safe and potent biological agent, there is scope for its use in cancer therapy in humans [38, 39]. However, the observed TRAIL resistance in certain cancer cells remains unclear. Autophagy is an alternative cell-death mechanism, and it plays an important role in recycling cellular components. Complete autophagic flux is a mechanism by which cellular components are recruited to lysosomes for degradation [40, 41]. Anti-malarial drugs such as CQ function as autophagy inhibitors and have been shown to impair autophagy in clinical trials for cancer therapy [42]. Recent studies suggested that autophagy inhibition sensitized cancer cells to apoptosis and a complete autophagic flux promoted cancer cell survival [43, 44].

A549 lung cancer cells are resistant to TRAIL [13, 45]. In the present study, we detected that desipramine or TRAIL alone was not capable of inducing cell death in A549 lung cancer cells. Notably, the combined treatment of desipramine and TRAIL strongly promoted cell death in A549 cells. Moreover, the combined treatment robustly inhibited colony formation and reduced size in A549 cells (Figures 1, 2). Desipramine, which upregulated DR5 expression, exerted this apoptotic effect, owing to the combined effect of TRAIL and desipramine (Figure 3). This experiment proposed that desipramine, in combination with TRAIL, played a role as an anti-cancer agent that could be used to sensitize lung cancer cells to TRAIL-induced apoptosis. Treatment with desipramine alone increased LC3-II and p62 levels in A549 cells in a dose-dependent manner.

Our findings showed that the inhibition of DR5 expression by DR5-specific siRNA abundantly increased cell viability and thus inhibited the effects of desipramine on TRAIL-mediated apoptosis. These results indicated that DR5 upregulation was required for the combined effect of desipramine and TRAIL. Moreover, these findings, for the first time, revealed that desipramine enhanced DR5 expression via autophagy inhibition (Figure 4). It was also revealed

 doi:10.20944/preprints202012.0376.v1

that desipramine increased autophagosome formation, as indicated by LC3-II accumulation, and inhibited lysosomal fusion with autophagosomes, thereby resulting in increased p62 levels. This confirmed the inhibition of autophagic flux (Figure 5). Furthermore, the combined treatment of TRAIL and desipramine or CQ, compared with single treatment regimens, increased cell death to a greater extent. The inhibition of autophagy by desipramine and the lysosomal inhibitor CQ increased DR5 expression level and improved TRAIL-mediated caspase-dependent apoptotic cell death. Our findings were confirmed by the amplified levels of the intracellular apoptosis-related proteins—activated caspase-3 and activated caspase-8 (Figures 6, 7).

In conclusion, we reported that desipramine treatment enhanced the function of TRAIL by upregulating DR5 expression. Moreover, the combined treatment of desipramine and TRAIL improved apoptosis in TRAIL-resistant A549 cells, indicating that desipramine treatment increased TRAIL-induced cancer cell death in TRAIL-resistant A549 lung cancer cells via inhibiting autophagic flux.

Preprints (www.preprints.org) | NOT PEER-REVIEWED | Posted: 15 December 2020 doi:10.20944/preprints202012.0376.v1

4. Materials and methods

4.1. Cells and culture systems: A549 and HCC-15 lung cancer cell line was acquired from the American Type Culture Collection (Global Bioresource Center, Manassas, VA, USA). Calu-3 cancer cells were purchased from the Korean Cell Line Bank (Korean Cell Line Research Foundation). Cells were cultured in Roswell Park Memorial Institute-1640 medium (Gibco BRL, Grand Island, NY, USA), supplemented with 10% (v/v) fetal bovine serum and antibiotics (100 µg/mL penicillin–streptomycin), at 37°C in a 5% CO_2 incubator.

4.2. Reagents: Desipramine and CQ were purchased from Sigma-Aldrich (St. Louis, MO, USA), and TRAIL (100 ng/mL) was purchased from AbFrontier (Geumcheon-gu, Seoul, the Republic of Korea).

4.3. Cell viability assay: Cell viability was assessed by methyl thiazolyltetrazolium (MTT) and crystal violet staining assays. Cells were plated in 12-well plates at a density of 1.0×10^4 cells/well and incubated at 37°C for 24 h. Cells were pretreated with different concentrations of desipramine for 12 h and then exposed to recombinant TRAIL (100 ng/mL) for 3 h. In addition, the cells were pretreated with CQ (20 µM) for 1 h and then treated with desipramine. Cell morphology was observed under an inverted microscope (Nikon, Tokyo, Japan). Cell viability was assessed by adding 5 mg/mL MTT (500 µL) to each well and incubating the plates at 37°C for 2 h. After incubation, the MTT solution was removed, and the wells were treated with dimethyl sulfoxide (500 µL). The absorbance was measured at 570 nm using a spectrophotometer (Bio-Rad, Hercules, CA, USA). For the crystal violet assay, cells were stained with a staining solution (0.5% crystal violet in 30% ethanol and 3% formaldehyde) at room temperature (25℃) for 10–20 min, washed 3–4 times with phosphate-buffered saline (PBS), and then imaged.

4.4. Trypan blue exclusion assay: The number of live cells was counted using microscopy and a hemocytometer after staining the cells with trypan blue (Sigma-Aldrich). The results were calculated as percentages and compared to those of the vehicle-treated controls.

4.5. Colony-formation assay: Cells were plated in 12-well plates and treated with the indicated doses of TRAIL and desipramine. After 2 days, the medium was replaced with new medium without TRAIL and desipramine and further cultured for a week. Colonies were fixed in 100% methanol for 20 min and stained with 0.05% (w/v) crystal violet for 5 min. After washing, colonies were counted under an inverted microscope (Nikon, Japan).

Preprints (www.preprints.org) | NOT PEER-REVIEWED | Posted: 15 December 2020 doi:10.20944/preprints202012.0376.v1

4.6. Flow cytometric analysis of apoptosis: Apoptosis was assessed by flow cytometry using an Annexin V Assay Kit (Santa Cruz Biotechnology, Santa Cruz, CA, USA), according to the manufacturer's protocol. Annexin V levels were determined by measuring fluorescence at 488 nm of excitation and 525/30 emission using a Guava easyCyteHT System (Millipore, Bedford, MA, USA).

4.7. Western blot assay: Cells were lysed in lysis buffer [25 mM HEPES (pH 7.4), 100 mM ethylenediaminetetraacetic acid, 5 mM $MgCl_2$, 0.1 mM dithiothreitol, and a protease inhibitor cocktail] and sonicated to prepare cell lysates. Equal amounts of proteins were separated by 10–15% sodium dodecyl sulfate-polyacrylamide gel electrophoresis and transferred onto nitrocellulose or polyvinylidene fluoride membranes. Cells were then blotted with the indicated concentrations of primary antibodies in a dilution buffer (1% milk with PBS-Tween) and then secondary antibodies (1:5,000), and the membranes were developed using enhanced chemiluminescence reagents. Primary antibodies such as DR5 (1:10,000; Abcam, Cambridge, MA, USA), DR4 (1:1,000; Abcam), LC3 (1:1,000; Sigma-Aldrich), p62 (Sigma-Aldrich), atg5 (Cell Signaling Technology, Danvers, MA, USA), cleaved caspase-3 (Cell Signaling Technology), cleaved caspase-8 (BD Pharmingen/BD Biosciences, San Jose, CA, USA), and β-actin (Sigma-Aldrich), were used at appropriate dilutions for immunoblotting. The bands were visualized using a Fusion-FX7 imaging system (Vilber Lourmat, Marne-la-Vallée, France).

4.8. Immunocytochemistry (ICC): Cells were grown on glass coverslips, treated with desipramine, washed with 1% PBS, and then fixed with 4% paraformaldehyde in PBS at room temperature for 15 min. They were then washed twice with ice-cold PBS and incubated in PBS containing 0.25% Triton X-100 at room temperature for 10 min. After incubation, the cells were washed thrice with PBS and blocked with 1% bovine serum albumin (BSA) in PBS-Tween for 30 min. The cells were then incubated with primary antibodies (anti-p62 and -DR4/5 diluted with 1% BSA in PBS-Tween) in a 5% CO_2 incubator for 3 h. After incubation, the cells were washed thrice with PBS. These cells were then incubated with secondary antibodies (diluted with 1% BSA in PBS-Tween) in the dark at room temperature for 2 h. The cells were washed with PBS 3–4 times. Next, they were treated with 4,6-diamidino-2-phenylindole and incubated for 10 min. Cells were washed thrice, mounted with fluorescent mounting medium, and then captured under a fluorescence microscope (#451203, Nikon ECLIPSE 80i; Nikon Corporation, Tokyo, Japan; magnification, ×400).

Preprints (www.preprints.org) | NOT PEER-REVIEWED | Posted: 15 December 2020 doi:10.20944/preprints202012.0376.v1

4.9. Transmission electron microscopy (TEM): Trypsinized cells were fixed with 2% glutaraldehyde (Electron Microscopy Sciences, Hatfield, PA, USA) in PBS and then 2% osmium tetroxide (Electron Microscopy Sciences) and dehydrated with ethanol at different concentrations (25, 50, 70, 90, and 100%) for 5 min each. The dehydrated samples were then embedded in epoxy resin (Embed 812; Electron Microscopy Sciences) at 60°C for 48 h, according to the manufacturers' instructions. Ultrathin sections (60 nm) were prepared using an LKB III ultratome (Leica Microsystems GmbH, Wetzlar, Germany) and stained with 0.5% uranyl acetate (Electron Microscopy Sciences) for 20 min and 0.1% lead citrate (Electron Microscopy Sciences) at room temperature for 7 min. Images were captured under a Hitachi H7650 electron microscope (Hitachi, Ltd., Tokyo, Japan; magnification, ×10,000) installed at the Center for University Wide Research Facilities at Jeonbuk National University.

4.10. Small interfering RNA (siRNA) transfection: Tested cell lines were transfected with siRNA using Lipofectamine (Invitrogen, CA, USA), according to the manufacturer's protocol. Knockdown proficiency was assessed by immunoblotting. The DR5-specific and scrambled control siRNA were purchased from Ambion, Life Technologies, CA, USA; atg5-specific siRNA and transfection reagent Lipofectamine 2000 were purchased from Invitrogen.

4.11. Quantitative reverse transcription polymerase chain reaction (qRT-PCR): mRNA transcripts of DR5 were measured by SYBR Green-based qRT-PCR. Total RNA was extracted from the cells using RiboEX (GeneAll Biotechnology, Korea). The extracts were then converted into cDNA using reverse transcriptase (Enzynomics, Korea) on a CFX96^{TM} Real-PCR Detection System (Bio-Rad Laboratories), following the manufacturer’s instructions. Gene primers (1 µL), with SYBR Green (Bio-Rad Laboratories) and a total reaction volume of 20 µL, were used for qRT-PCR. The sequences of the primers used were DR5 (forward: 5'-GCGGTCCTGCTGTTGGTCTC-3', reverse: 5'-GCTTCTGTCCACACGCTCAG-3') and GAPDH, which was used as an internal control (forward: 5'-TGCACCACCAACTGCTTAG-3', reverse: 5'-GGATGCAGGGATGATGTT-3'). All data were evaluated using Bio-Rad CFX manager version 2.1 analysis software (Bio-Rad Laboratories).

4.12. Statistical analysis: The data are expressed as the mean ± standard deviation (SD). The significance of the differences between treatments was determined using one-way analysis of variance (ANOVA), followed by the Tukey–Kramer test. Statistical analyses were performed using the GraphPad Prism 5 software (GraphPad Software, Inc.). A p-value <0.05 was

 doi:10.20944/preprints202012.0376.v1

considered significant.

 doi:10.20944/preprints202012.0376.v1

Declarations

Authors' contributions: KZ and SP designed and performed the study, and KZ, JS and SP analyzed data and wrote the manuscript. All authors have read and approved the final manuscript.

Funding: This study was supported by a grant from National Research Foundation of the Korea (NRF) funded by the Ministry of Education (grant no. 2019R1A6A1A03033084) and "Research Base Construction Fund Support Program" funded by Jeonbuk National University in 2020.

Acknowledgements: Not applicable.

Conflicts of Interest: The authors declare no conflict of interest.

Abbreviations:

CQ	Chloroquine
DISC	Death-inducing signaling complex
DR /5	Death receptor 4/5
FADD	Fas-associated death domain
ICC	Immunocytochemistry
LC3	Microtubule-associated protein light chain 3
MTT	Methyl thiazolyltetrazolium
siRNA	Small interfering RNA
TCA	Tricyclic antidepressant
TEM	Transmission electron microscopy
TRAIL	Tumor necrosis factor-related apoptosis-inducing ligand

 doi:10.20944/preprints202012.0376.v1

References

1. Dela Cruz, C.S., L.T. Tanoue, and R.A. Matthay, *Lung cancer: epidemiology, etiology, and prevention.* Clinics in chest medicine, 2011. **32**(4): p. 605-644.
2. Siegel, R.L., K.D. Miller, and A. Jemal, *Cancer statistics, 2019.* CA: a cancer journal for clinicians, 2019. **69**(1): p. 7-34.
3. Hirsch, F.R., et al., *Lung cancer: current therapies and new targeted treatments.* Lancet (London, England), 2017. **389**(10066): p. 299-311.
4. Huang, C.-Y., et al., *A review on the effects of current chemotherapy drugs and natural agents in treating non-small cell lung cancer.* BioMedicine, 2017. **7**(4): p. 23-23.
5. Bayat Mokhtari, R., et al., *Combination therapy in combating cancer.* Oncotarget, 2017. **8**(23): p. 38022-38043.
6. Valley, C.C., et al., *Tumor necrosis factor-related apoptosis-inducing ligand (TRAIL) induces death receptor 5 networks that are highly organized.* The Journal of biological chemistry, 2012. **287**(25): p. 21265-21278.
7. Griffith, T.S., et al., *TRAIL gene therapy: from preclinical development to clinical application.* Current gene therapy, 2009. **9**(1): p. 9-19.
8. Fossati, S., J. Ghiso, and A. Rostagno, *TRAIL death receptors DR4 and DR5 mediate cerebral microvascular endothelial cell apoptosis induced by oligomeric Alzheimer's Aβ.* Cell death & disease, 2012. **3**(6): p. e321-e321.
9. Wang, S. and W.S. El-Deiry, *TRAIL and apoptosis induction by TNF-family death receptors.* Oncogene, 2003. **22**(53): p. 8628-8633.
10. Dai, X., et al., *Targeting TNF-related apoptosis-inducing ligand (TRAIL) receptor by natural products as a potential therapeutic approach for cancer therapy.* Experimental biology and medicine (Maywood, N.J.), 2015. **240**(6): p. 760-773.
11. Zhang, L. and B. Fang, *Mechanisms of resistance to TRAIL-induced apoptosis in cancer.* Cancer gene therapy, 2005. **12**(3): p. 228-237.
12. Huang, Y., et al., *Overcoming resistance to TRAIL-induced apoptosis in solid tumor cells by simultaneously targeting death receptors, c-FLIP and IAPs.* International journal of oncology, 2016. **49**(1): p. 153-163.
13. Guo, Z.L., et al., *Shikonin sensitizes A549 cells to TRAIL-induced apoptosis through the JNK, STAT3 and AKT pathways.* BMC cell biology, 2018. **19**(1): p. 29-29.
14. Li, X., et al., *Reversal of the Apoptotic Resistance of Non-Small-Cell Lung Carcinoma towards TRAIL by Natural Product Toosendanin.* Scientific reports, 2017. **7**: p. 42748-42748.
15. Trivedi, R. and D.P. Mishra, *Trailing TRAIL Resistance: Novel Targets for TRAIL Sensitization in*

Cancer Cells. Frontiers in oncology, 2015. **5**: p. 69-69.

16. Yonekawa, T. and A. Thorburn, *Autophagy and cell death.* Essays in biochemistry, 2013. **55**: p. 105-117.
17. Kroemer, G., G. Mariño, and B. Levine, *Autophagy and the integrated stress response.* Molecular cell, 2010. **40**(2): p. 280-293.
18. Yu, L., Y. Chen, and S.A. Tooze, *Autophagy pathway: Cellular and molecular mechanisms.* Autophagy, 2018. **14**(2): p. 207-215.
19. Tanida, I., T. Ueno, and E. Kominami, *LC3 and Autophagy.* Methods in molecular biology (Clifton, N.J.), 2008. **445**: p. 77-88.
20. Ma, S., I.Y. Attarwala, and X.-Q. Xie, *SQSTM1/p62: A Potential Target for Neurodegenerative Disease.* ACS chemical neuroscience, 2019. **10**(5): p. 2094-2114.
21. Zhang, Z., R. Singh, and M. Aschner, *Methods for the Detection of Autophagy in Mammalian Cells.* Current protocols in toxicology, 2016. **69**: p. 20.12.1-20.12.26.
22. Kung, C.-P., et al., *Autophagy in tumor suppression and cancer therapy.* Critical reviews in eukaryotic gene expression, 2011. **21**(1): p. 71-100.
23. Russo, M. and G.L. Russo, *Autophagy inducers in cancer.* Biochemical pharmacology, 2018. **153**: p. 51-61.
24. Bhat, P., et al., *Modulating autophagy in cancer therapy: Advancements and challenges for cancer cell death sensitization.* Biochemical pharmacology, 2018. **147**: p. 170-182.
25. Zhang, X., et al., *Blocking Autophagy in Cancer-Associated Fibroblasts Supports Chemotherapy of Pancreatic Cancer Cells.* Frontiers in Oncology, 2018. **8**(590).
26. Zinnah, K.M.A. and S.-Y. Park, *Duloxetine Enhances TRAIL-mediated Apoptosis via AMPK-mediated Inhibition of Autophagy Flux in Lung Cancer Cells.* Anticancer research, 2019. **39**(12): p. 6621-6633.
27. Qiao, X., et al., *Azithromycin enhances anticancer activity of TRAIL by inhibiting autophagy and up-regulating the protein levels of DR4/5 in colon cancer cells in vitro and in vivo.* Cancer communications (London, England), 2018. **38**(1): p. 43-43.
28. Mauthe, M., et al., *Chloroquine inhibits autophagic flux by decreasing autophagosome-lysosome fusion.* Autophagy, 2018. **14**(8): p. 1435-1455.
29. Levy, J.M.M., C.G. Towers, and A. Thorburn, *Targeting autophagy in cancer.* Nature reviews. Cancer, 2017. **17**(9): p. 528-542.
30. Onorati, A.V., et al., *Targeting autophagy in cancer.* Cancer, 2018. **124**(16): p. 3307-3318.
31. Ostuzzi, G., et al., *Antidepressants for the treatment of depression in people with cancer.*The Cochrane database of systematic reviews, 2018. **4**(4): p. CD011006-CD011006.

32. Deng, L., et al., *Prophylactic treatment with the tricyclic antidepressant desipramine prevents development of paclitaxel-induced neuropathic pain through activation of endogenous analgesic systems.* Pharmacological research, 2016. **114**: p. 75-89.
33. Lu, T., et al., *Desipramine-induced Ca-independent apoptosis in Mg63 human osteosarcoma cells: dependence on P38 mitogen-activated protein kinase-regulated activation of caspase 3.* Clinical and experimental pharmacology & physiology, 2009. **36**(3): p. 297-303.
34. Arimochi, H. and K. Morita, *Desipramine induces apoptotic cell death through nonmitochondrial and mitochondrial pathways in different types of human colon carcinoma cells.* Pharmacology, 2008. **81**(2): p. 164-172.
35. Chang, H.-C., et al., *Desipramine-induced apoptosis in human PC3 prostate cancer cells: activation of JNK kinase and caspase-3 pathways and a protective role of [Ca2+]i elevation.* Toxicology, 2008. **250**(1): p. 9-14.
36. Ma, J., et al., *Desipramine induces apoptosis in rat glioma cells via endoplasmic reticulum stress-dependent CHOP pathway.* Journal of neuro-oncology, 2011. **101**(1): p. 41-48.
37. Kinjo, T., et al., *Effects of desipramine on the cell cycle and apoptosis in Ca3/7 mouse skin squamous carcinoma cells.* International journal of molecular medicine, 2010. **25**(6): p. 861-867.
38. de Miguel, D., et al., *Onto better TRAILs for cancer treatment.* Cell death and differentiation, 2016. **23**(5): p. 733-747.
39. Lemke, J., et al., *Getting TRAIL back on track for cancer therapy.* Cell Death & Differentiation, 2014. **21**(9): p. 1350-1364.
40. Ganley, I.G., et al., *Distinct autophagosomal-lysosomal fusion mechanism revealed by thapsigargin-induced autophagy arrest.* Molecular cell, 2011. **42**(6): p. 731-743.
41. Pugsley, H.R., *Assessing Autophagic Flux by Measuring LC3, p62, and LAMP1 Co-localization Using Multispectral Imaging Flow Cytometry.* Journal of visualized experiments : JoVE, 2017(125): p. 55637.
42. Marinković, M., et al., *Autophagy Modulation in Cancer: Current Knowledge on Action and Therapy.* Oxidative medicine and cellular longevity, 2018. **2018**: p. 8023821-8023821.
43. Fitzwalter, B.E., et al., *Autophagy Inhibition Mediates Apoptosis Sensitization in Cancer Therapy by Relieving FOXO3a Turnover.* Developmental cell, 2018. **44**(5): p. 555-565.e3.
44. Pan, H., et al., *Autophagic flux disruption contributes to Ganoderma lucidum polysaccharide-induced apoptosis in human colorectal cancer cells via MAPK/ERK activation.* Cell Death & Disease, 2019. **10**(6): p. 456.
45. Nazim, U.M., et al., *Enhancement of TRAIL-induced apoptosis by 5-fluorouracil requires*

 doi:10.20944/preprints202012.0376.v1

activating Bax and p53 pathways in TRAIL-resistant lung cancers. Oncotarget, 2017. **8**(11): p. 18095-18105.

Preprints (www.preprints.org) | NOT PEER-REVIEWED | Posted: 15 December 2020 doi:10.20944/preprints202012.0376.v1

Figure Legends

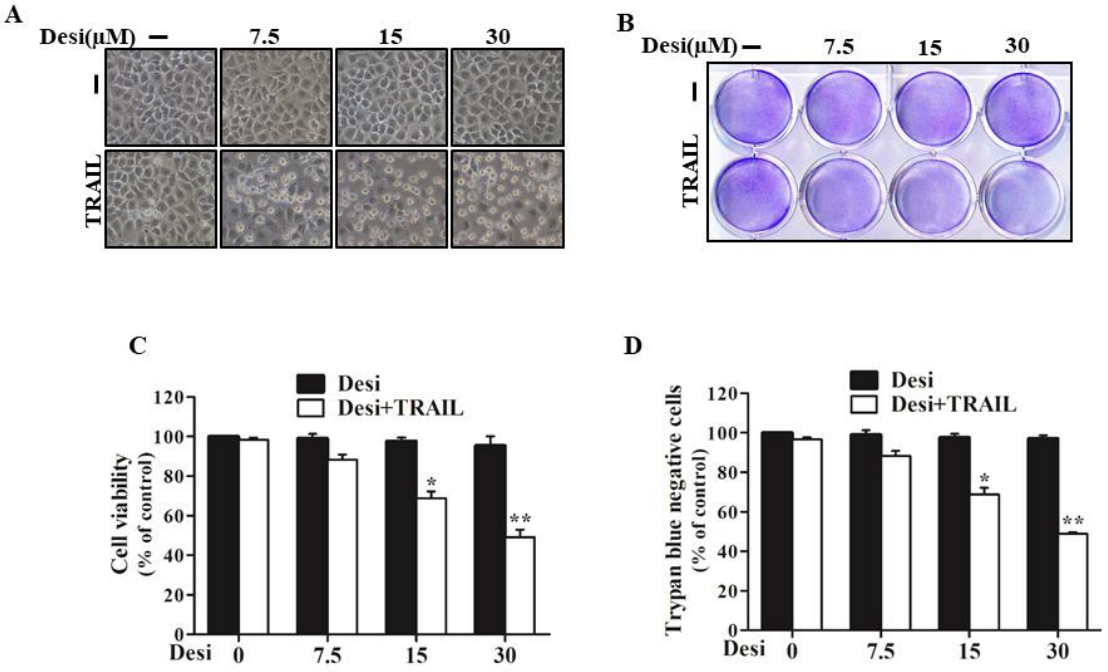

Figure 1

Preprints (www.preprints.org) | NOT PEER-REVIEWED | Posted: 15 December 2020 doi:10.20944/preprints202012.0376.v1

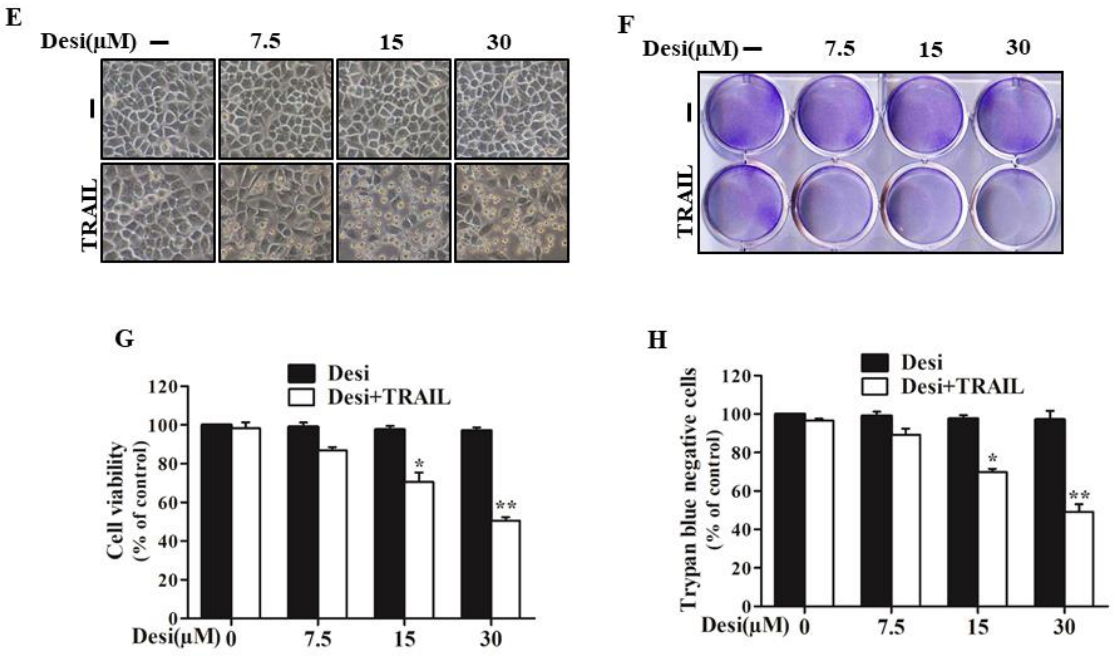

Figure 1

Preprints (www.preprints.org) | NOT PEER-REVIEWED | Posted: 15 December 2020 doi:10.20944/preprints202012.0376.v1

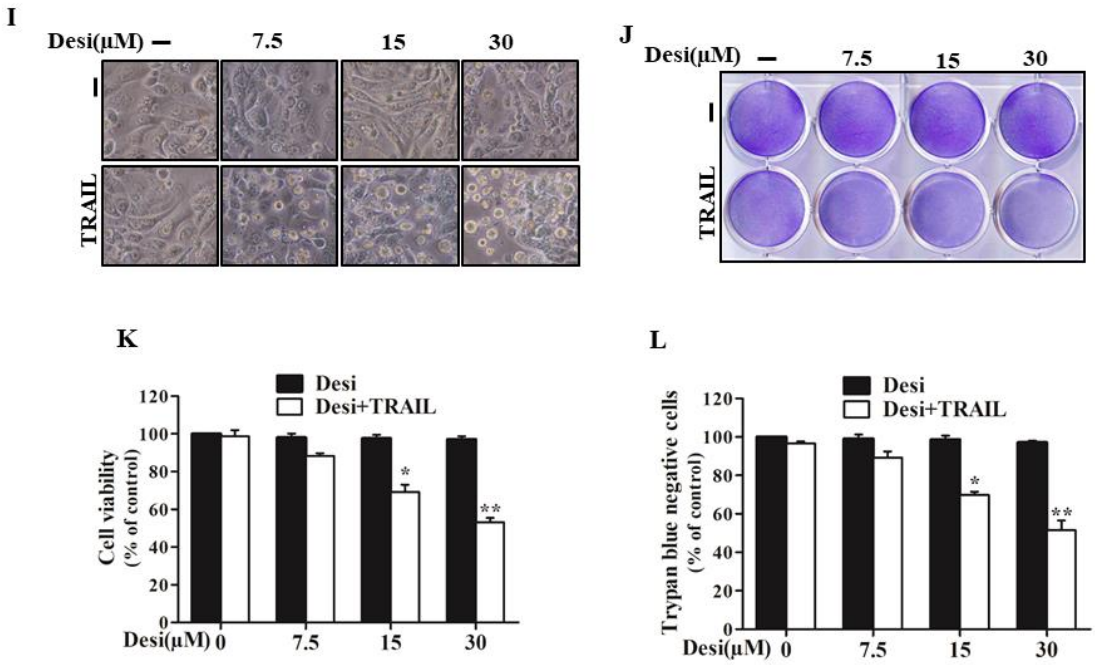

Figure 1

Figure 1. Effects of desipramine treatment on TRAIL-induced apoptosis of lung cancer cells. (A-D) A549, (E-H) HCC-15 and (I-L) Calu-3 cells were preincubated with designated concentrations of desipramine for 12 h and then with TRAIL (100 ng/mL) for 3 h. (A, E and I) Cells were photographed, and variations in morphology were examined under a light microscope (×100). (B, F and J) Mean density of crystal violet stained A549 cells is shown. (C, G and K) MTT assays were conducted to analyze cell viability, as represented by a bar graph. (D, H and L) Viable cells were counted by trypan blue exclusion assay. Statistically significant differences between the control and each indicated treatment group are shown as *p <0.01 and **p <0.001. Desi: desipramine; TRAIL: tumor necrosis factor-related apoptosis-inducing ligand

Preprints (www.preprints.org) | NOT PEER-REVIEWED | Posted: 15 December 2020 doi:10.20944/preprints202012.0376.v1

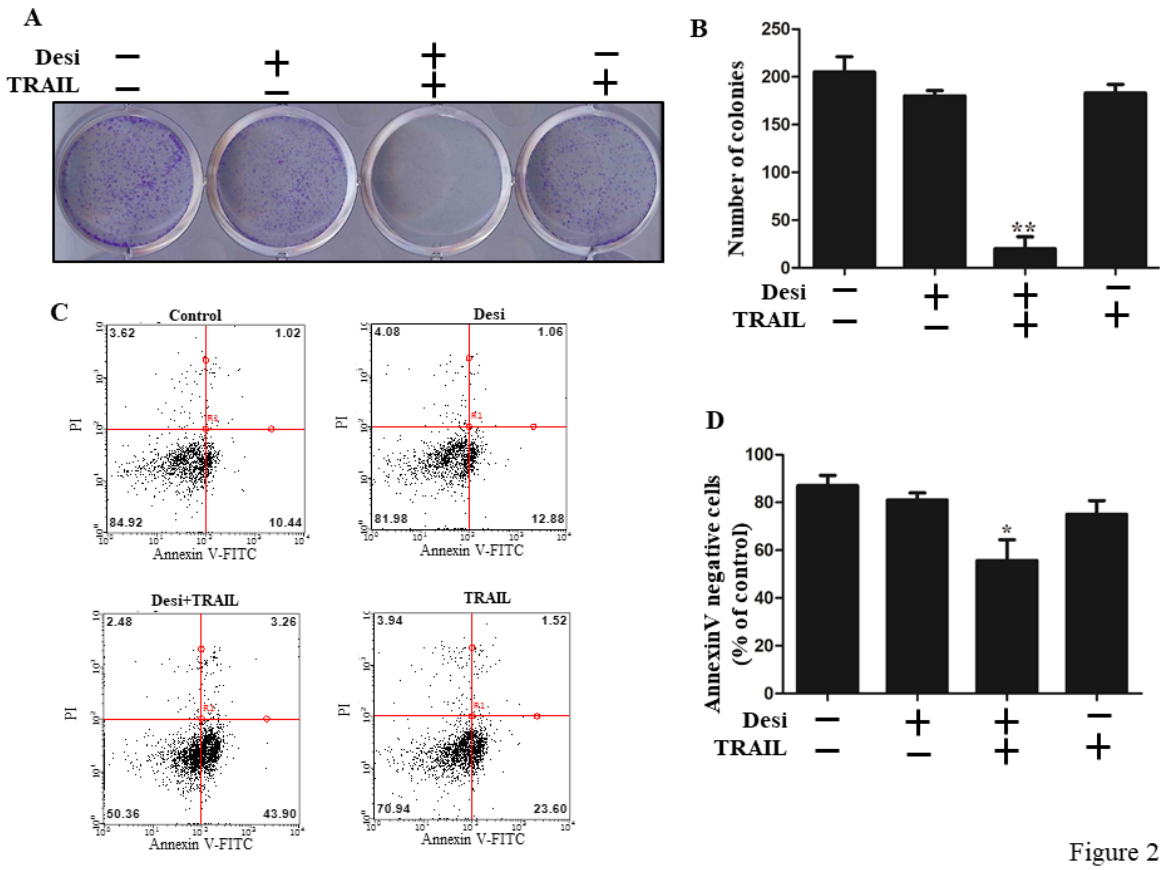

Figure 2. Combined desipramine and TRAIL inhibits colony formation and enhances TRAIL-mediated apoptosis. Colony formation and apoptosis test was performed to observe the colony formation ability and apoptosis of A549 cells treated with desipramine, TRAIL, or combined desipramine and TRAIL. (A, B) A549 cells were cultured with the indicated doses of desipramine and/or TRAIL. After 24 h, the medium was replaced with new medium without drugs and further cultured for a week. Colonies were stained with crystal violet dye and counted. (C, D) Cells were pretreated with desipramine (30 μM) for 12 h and then treated with TRAIL (100 ng/mL) for an additional 2 h 30 min. Apoptosis was assessed by annexin V assay after using 1:1 fluorescein isothiocyanate and propidium iodide reagents. Statistically significant differences between the control and each indicated treatment group are shown as $*p < 0.05$ and $**p < 0.001$. The results represent the mean of at least three independent experiments.

Preprints (www.preprints.org) | NOT PEER-REVIEWED | Posted: 15 December 2020 doi:10.20944/preprints202012.0376.v1

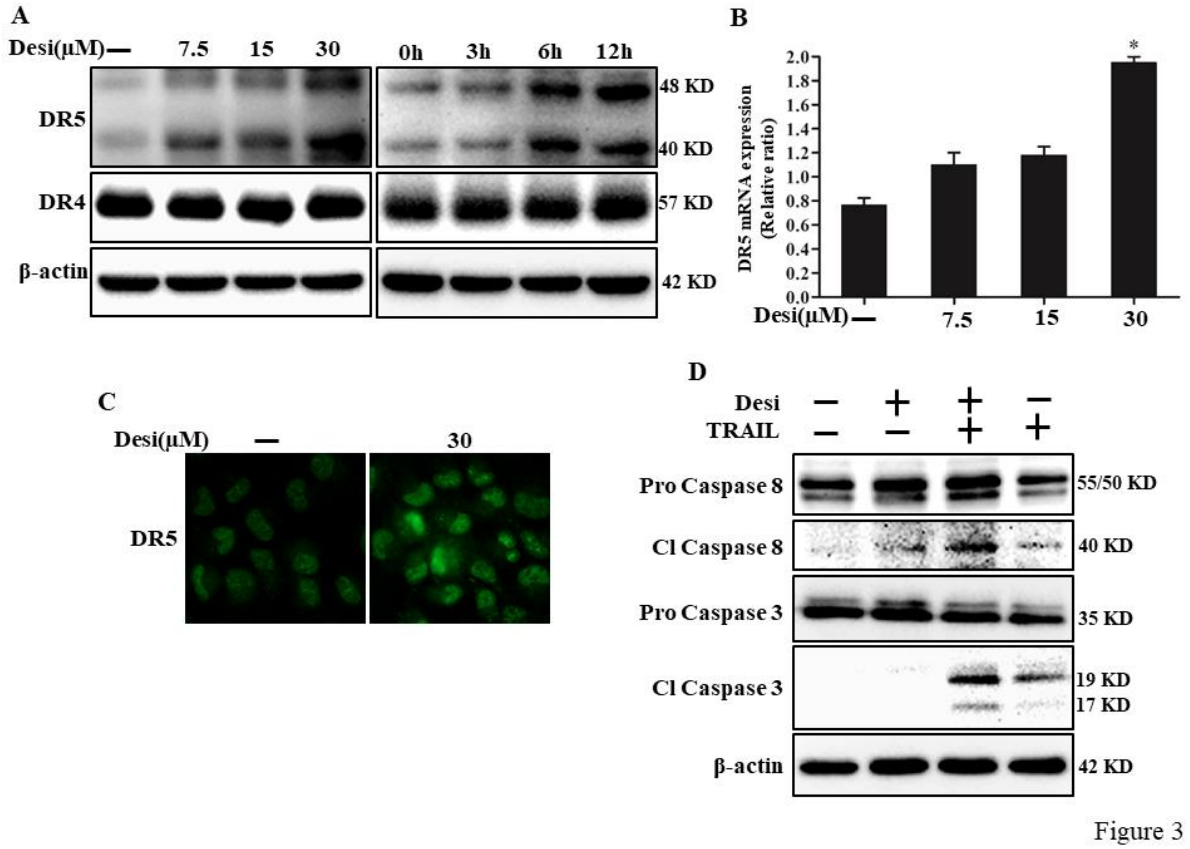

Figure 3

Figure 3. Effects of TRAIL receptor-2 (DR5) on TRAIL-induced apoptosis. A549 cells were preincubated with designated doses of desipramine for 12 h. (A) Harvested cell lysates were collected and subjected to western blot analysis to measure DR4 and DR5 expression levels. (B) DR5 mRNA expression was assessed by qRT-PCR. (C) ICC revealed substantial DR5 expression in desipramine-treated cells. (D) Desipramine (30 μM)-treated cells were incubated for 12 h and then exposed to TRAIL (100 ng/mL) for 3 h. The intracellular apoptosis regulatory proteins, cleaved caspase-8 and cleaved caspase-3, were detected by immunoblot analysis. Statistically significant differences between the control and each indicated treatment group are shown as $*p < 0.001$.

Preprints (www.preprints.org) | NOT PEER-REVIEWED | Posted: 15 December 2020 doi:10.20944/preprints202012.0376.v1

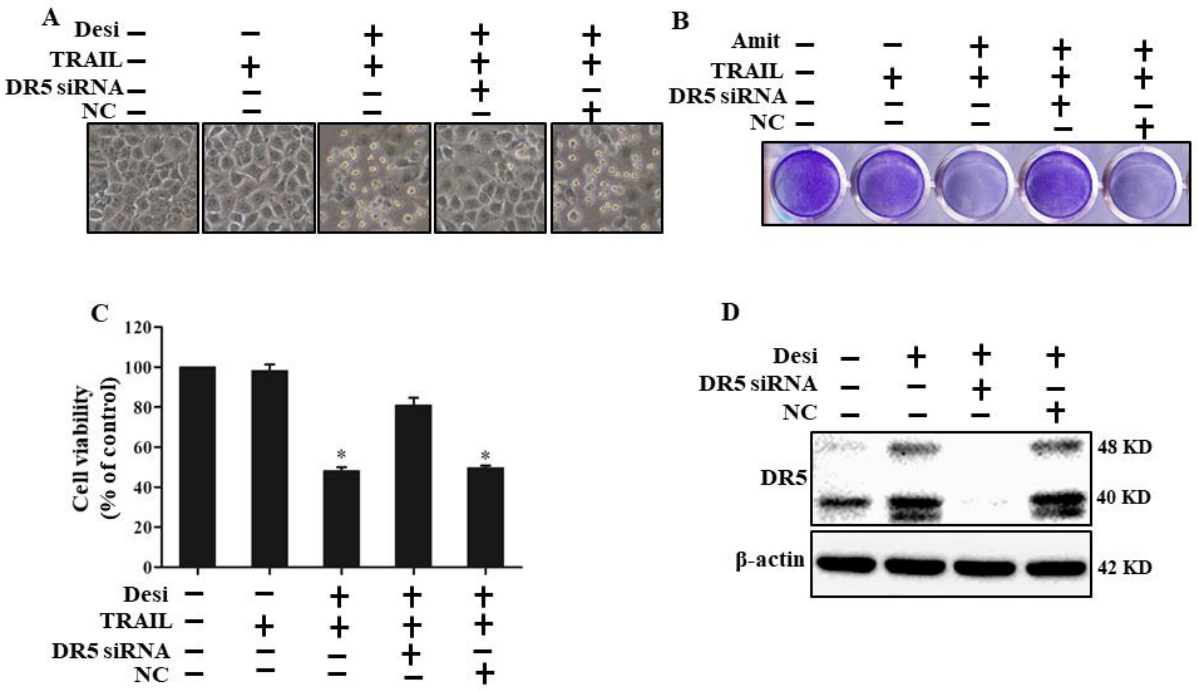

Figure 4

Figure 4. Suppression of DR5 reverses desipramine-induced TRAIL-mediated apoptosis. DR5-specific siRNA and NC siRNA (40 nM) were transfected into cells for 24 h. The cells were then treated with desipramine (30 μM) for 12 h and finally exposed to TRAIL (100 ng/mL) for 3 h. (A) Cells were photographed, and morphological variations were examined under a light microscope (×100). (B) Mean density of crystal violet stained A549 cells is shown. (C) MTT assays were conducted to calculate cell viability percentages, as represented by a bar diagram. Statistically significant differences between the control and each indicated treatment group are shown as $*p < 0.001$. (D) Cell lysates were harvested and subjected to western blot analysis to determine DR5 expression. β-actin was used as a loading control.

Preprints (www.preprints.org) | NOT PEER-REVIEWED | Posted: 15 December 2020 doi:10.20944/preprints202012.0376.v1

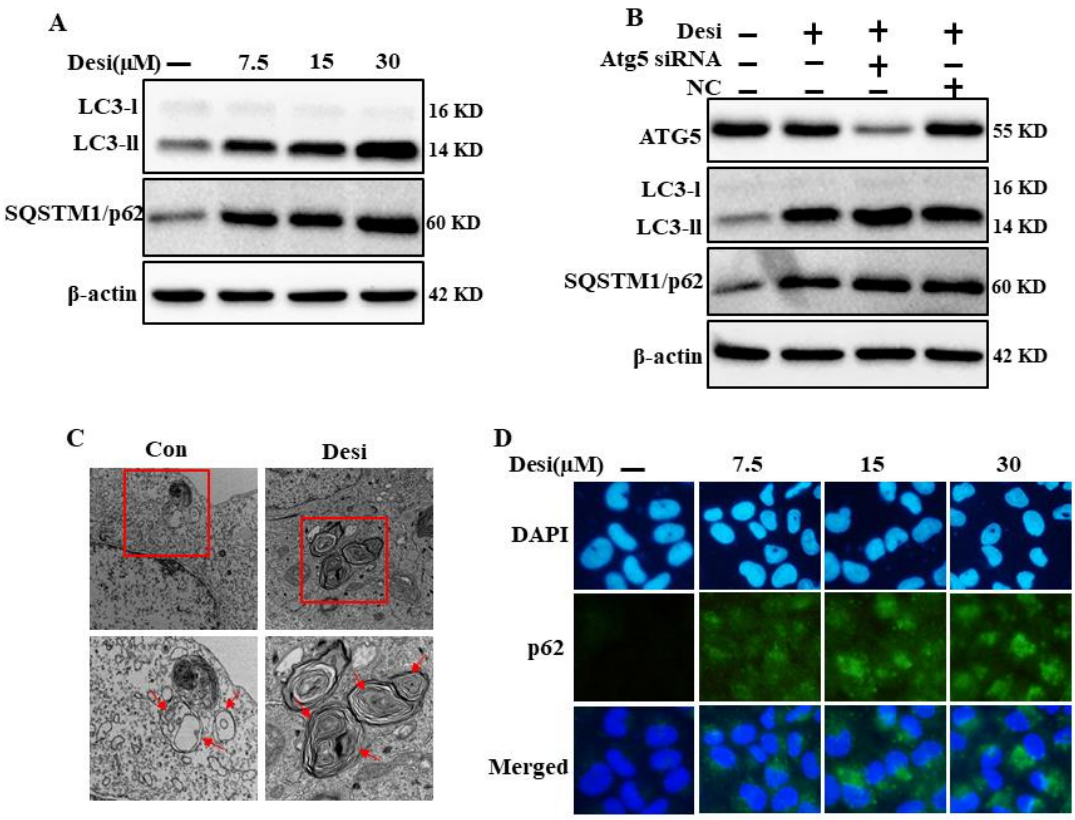

Figure 5

Figure 5. Effects of desipramine treatment on autophagic flux. A549 cells were incubated with designated doses of desipramine for 12 h. (A) Expression levels of LC3-II and p62 were analyzed by western blotting. (B) p62 expression on desipramine treatment was analyzed by ICC. (C) TEM showed accumulation of autophagosomes.

Preprints (www.preprints.org) | NOT PEER-REVIEWED | Posted: 15 December 2020 doi:10.20944/preprints202012.0376.v1

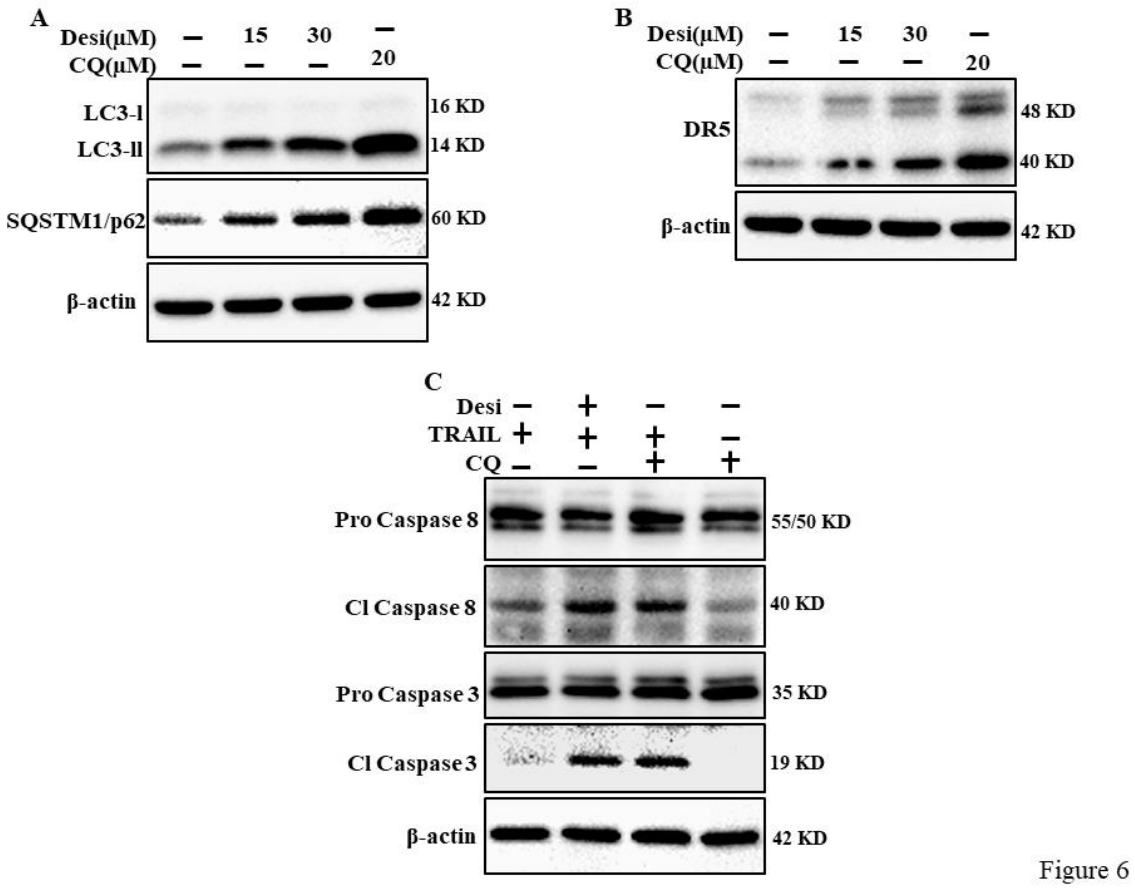

Figure 6

Figure 6. Autophagic flux inhibition upregulates DR5. Cells were preincubated with CQ (20 μM) and different doses of desipramine for 12 h. (A) LC3-II and p62 expression levels were evaluated by western blotting. (B) DR5 expression was assessed by immunoblotting. (C) Cells were preincubated with desipramine (30 μM) or CQ for 12 h and then treated with TRAIL (100 ng/mL) for 2 h. Western blotting technique was applied to evaluate the expression levels of cleaved caspase-8 and cleaved caspase-3.

Preprints (www.preprints.org) | NOT PEER-REVIEWED | Posted: 15 December 2020 doi:10.20944/preprints202012.0376.v1

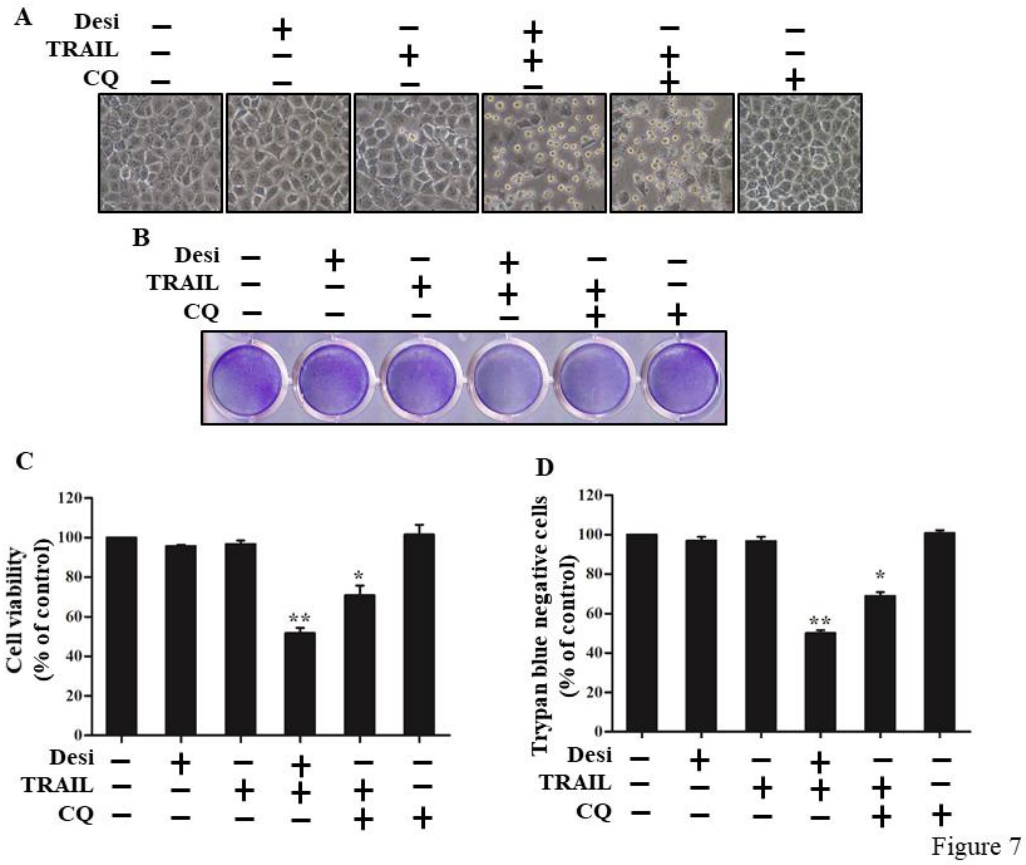

Figure 7

Figure 7. Autophagy inhibition by desipramine augments TRAIL-induced cell death. Cells were preincubated with or without CQ (20 μM) and desipramine (30 μM) for 12 h and finally exposed to TRAIL (100 ng/mL) for 3 h. (A) Cell morphology was captured under a light microscope (×100). (B) Mean density of crystal violet stained A549 cells is shown. (C) MTT assays were conducted to analyze cell viability, as represented by a bar diagram. (D) Viable cells were counted by trypan blue exclusion assay. Statistically significant differences between the control and each indicated treatment group are shown as $*p < 0.01$ and $**p < 0.001$. CQ: chloroquine.